SH-Stretching Vibrational Spectra of Ethanethiol and *tert*-Butylthiol

Benjamin J. Miller, Daryl L. Howard,† Joseph R. Lane, and Henrik G. Kjaergaard*

Department of Chemistry, University of Otago, P.O. Box 56, Dunedin, New Zealand

Meghan E. Dunn and Veronica Vaida

Department of Chemistry and Biochemistry and CIRES, University of Colorado, Campus Box 215, Boulder, Colorado 80309, USA

Received: February 24, 2009; Revised Manuscript Received: April 16, 2009

Vibrational spectra of vapor-phase ethanethiol and *tert*-butylthiol have been recorded in the 1000 to 12 000 cm^{-1} region. Both the gauche and trans conformers of ethanethiol are observed. The intensities of SH-stretching vibrations are found to be significantly weaker than the equivalent CH-stretching vibrations and the OH-stretching vibrations in the corresponding alcohols. The relative strength of the SH-stretching vibrations in ethanethiol and *tert*-butylthiol compared with the OH-stretching vibrations in the corresponding alcohols are ~0.2 in the fundamental region and ~0.03 in the overtone regions. The SH- and OH-stretching intensities have been modeled with an anharmonic oscillator local mode model with ab initio calculated dipole moment functions. The weak nature of SH-stretching transitions is shown to be a result of both low anharmonicity of the vibrational mode and relatively small dipole moment derivatives.

Introduction

Vibrational spectra in the near-infrared (NIR) and visible regions are dominated by XH-stretching overtone transitions, where X is a heavy atom like C, O, or N.[1−3] The large amplitude motion associated with XH-stretching vibrations has been explained well by the anharmonic oscillator (AO) local mode model and for coupled XH-stretching oscillators by the harmonically (HCAO) or anharmonically (ACAO) coupled anharmonic oscillator coupled local mode models.[4−9] Calculation and experimental determination of absolute intensities is difficult. Transition frequencies can be measured very accurately, but transition intensities rely on several experimental parameters and are difficult to obtain quantitatively. Likewise, theoretically, transition frequencies can be calculated precisely solely from the molecular Hamiltonian, whereas transition intensities require both energies and wave functions from the molecular Hamiltonian as well as dipole moment functions.

There have been a number of studies that have compared calculated and measured absolute oscillator strengths of CH- and OH-stretching vibrational overtone transitions [for example refs 7, 10−18] and more recently on OH-stretching transitions in molecules of atmospheric interest.[19−25] These have mostly been based on AO and HCAO local mode models combined with empirical or ab initio calculated dipole moment functions in the internal local coordinates and either experimentally determined or ab initio calculated local mode parameters. We have shown for a few molecules that overtone intensities calculated with hybrid density functional theories (e.g., B3LYP) give results that are very similar to those obtained with correlated wave function-based methods.[26−28] More recently, the computationally expensive coupled cluster with single, double, and perturbative triple excitations [CCSD(T)] theory has been shown to accurately predict observed vibrational spectra when reasonable-sized basis sets are used.[25,29,30]

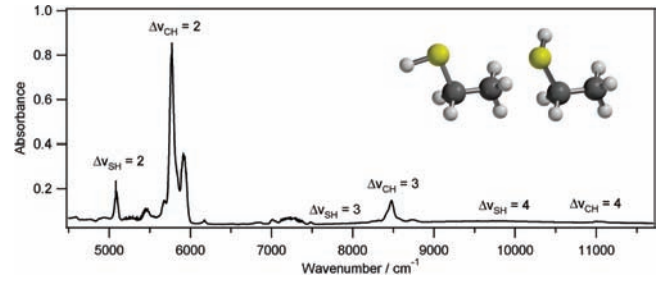

Figure 1. Near-infrared spectrum of ethanethiol recorded with a 71.4 cm cell and a pressure of 460 Torr. The inset figures show the CCSD(T)/aug-cc-pV(T+d)Z optimized geometries of the trans (left) and gauche (right) conformers.

Significantly fewer studies have been done on NH-stretching overtone transitions[31−34] and for SH-stretching transitions only a handful of studies on hydrogen sulfide (H_2S) have been completed.[35−37] It is usually difficult to handle molecules containing SH bonds as they have a foul smell and furthermore the intensities of the SH-stretching transitions in H_2S are significantly lower than those in H_2O. This reduced intensity is at least in part expected from the lower anharmonicity of the SH-stretching oscillator compared to the OH-stretching oscillator.

In this work, the SH-stretching fundamental and overtone transitions of vapor-phase ethanethiol (CH_3CH_2SH) and *tert*-butylthiol [$(CH_3)_3CSH$] were recorded to study the origin of the reduced intensity of SH-stretching vibrations. There have been few vapor-phase infrared studies of alkanethiols[38−43] and to our knowledge there are none on SH-stretching overtone vibrations. Ethanethiol exists at room temperature in two stable conformers, trans (C_S point group) and gauche (C_1 point group), whereas *tert*-butylthiol (C_S point group) has only one stable conformation. The structures of these conformers are depicted in the inset of Figures 1 and 2.

* To whom correspondence should be addressed. E-mail: henrik@alkali.otago.ac.nz. Fax: 64-3-479-7906. Tel.: 64-3-479-5378.

† Present address: Australian Synchrotron, 800 Blackburn Rd., Clayton, Victoria 3168, Australia.

10.1021/jp9017162 CCC: $40.75
Published on Web 05/11/2009

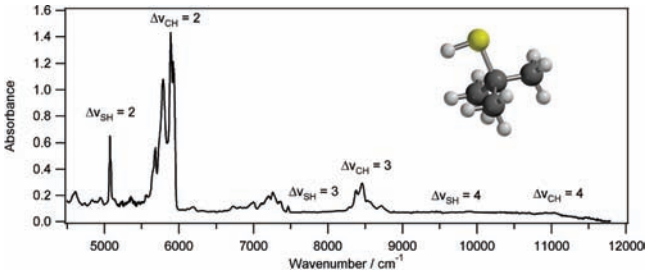

Figure 2. Near-infrared spectrum of *tert*-butylthiol recorded with a 14.25 m cell and a pressure of 35 Torr. The inset figure shows the CCSD(T)/aug'-cc-pV(T+d)Z optimized geometry.

Two Q-branches of differing intensity have been observed in the infrared spectrum of vapor-phase ethanethiol, split by 9 cm^{-1}.[38] The lower-frequency component of the SH-stretching band is assigned as being of the gauche conformer based on intensity arguments. Assuming similar cross sections, the intensity ratio of the CH_2 rocking mode is used to estimate the ratio between gauche and trans conformers, which is on the order of 3:1. In agreement with this assignment, theoretical results predict that the gauche conformer is the most populated.[43−48] Earlier infrared spectra at lower resolution could only identify one conformer.[39,42] The energy difference between the gauche and trans conformers of ethanethiol was estimated from its thermodynamic properties to be around 0.3 kcal mol^{-1} (∼100 cm^{-1}).[43,49]

Alongside infrared studies, there have also been Raman studies of ethanethiol.[45,50] Only one conformer is assigned in the SH-stretching fundamental Raman spectrum with a transition frequency at 2590 cm^{-1}, with an unassigned band observed at 2598 cm^{-1}.[45] It is interesting to note that Raman spectra of SH-stretching modes generally show quite high intensities.[51] This is probably due to the diffuse nature of the valence electrons on the sulfur atom.

Microwave spectra of both ethanethiol and *tert*-butylthiol have been studied extensively for different reasons. Ethanethiol has been studied for its challenging asymmetric rotor characteristics,[52−54] and both experimentally derived structural parameters and dipole moments have been reported. *tert*-Butylthiol has been studied because of its resemblance to a large symmetric top.[55,56]

Theoretical studies of alkanethiols often focus on the ability of various methods in molecular mechanics and quantum mechanics to model compounds that feature sulfur substituents. Although there have been numerous previous theoretical studies, there is a relative lack of modern theoretical work published on alkanethiols.[46,47,57−60] The MM4 force field calculations found the gauche conformer of ethanethiol to be 0.39 kcal mol^{-1} lower in enthalpy than the trans conformer.[44] Very recently, Choi et al. published work on both ethanethiol and *tert*-butylthiol.[48] They performed B3LYP/6-311++G(2df,2pd) geometry optimizations and frequency calculations on the gauche ($\Delta E = 0$ cm^{-1}) and trans ($\Delta E = 168$ cm^{-1}) conformers of ethanethiol and a single conformer of *tert*-butylthiol. Choi et al. also performed jet-cooled vacuum-ultraviolet mass analyzed threshold ionization (VUV-MATI) spectroscopy on these compounds. The low temperature of their experimental setup means that the single conformer of *tert*-butylthiol and only gauche ethanethiol were identified in their VUV-MATI spectra.

The aim of this article is to characterize the experimental SH-stretching vibrational spectrum of ethanethiol and *tert*-butylthiol within the framework of an anharmonic oscillator local mode model. We directly compare and contrast ethanethiol and *tert*-butylthiol to the analogous OH-containing molecules ethanol and *tert*-butanol.

Experimental Section

Ethanethiol (Fluka, ≥97%) and *tert*-butylthiol (2-methyl-2-propanethiol, Aldrich, 99%) were dried with molecular sieves and degassed with multiple freeze−pump−thaw cycles performed on a vacuum line before use. Experimental work was carried out at the University of Colorado, Boulder and at the University of Otago, Dunedin.

At Boulder, the vapor-phase spectra were recorded on a Bruker IFS 66v/S FTIR at 1 cm^{-1} resolution. The spectra were recorded with a gas cell having CaF_2 windows and a path length of either 15 or 71.4 cm. Spectra were recorded in the mid-infrared from 1000 to 8000 cm^{-1} with a Globar source, KBr beamsplitter, and MCT detector, and in the near-infrared from 2500 cm^{-1} to 11 700 cm^{-1} with a tungsten source, CaF_2 beamsplitter, and InSb detector. For comparison, IR and NIR spectra of ethanol (Pharmaco-Aaper, 99.98%) were also recorded. All vapor pressures were monitored using a piezo resistive vacuum sensor (Hastings HPM-760S) coupled to a vacuum gauge (Hastings THPM-760+). Cavity ringdown (CRD) experiments were performed in an attempt to observe the $\Delta v_{SH} = 4$ and $\Delta v_{SH} = 5$ overtones but were unsuccessful due to wavelength limitations of the instrument. However, the $\Delta v_{CH} = 5$ overtone of *tert*-butylthiol was recorded with the CRD. Cavity ring down is a highly sensitive spectroscopic method that uses two highly reflective mirrors ($R = 0.99999$) at either end of a cavity to produce a path length orders of magnitude greater than the cell.[61] For our 93.5 cm cell, the effective path length is ∼30 km for the $\Delta v_{SH} = 4$ region.

At Otago, spectra in the IR region from 1000 to 7500 cm^{-1} were recorded either with a 10 cm path length cell or a 4.8 m path length, multipass gas cell (Infrared Analysis Inc.) on a PerkinElmer Spectrum 100 FTIR spectrometer with a Quartz/halogen source, a KBr beamsplitter, and a FR-DTGS detector. The spectra in the NIR region from 4500 to 12 000 cm^{-1} were recorded with a variable path length Wilks gas cell, set at 14.25 m, on a Cary 500 spectrophotometer. The Cary spectra were recorded with the spectrometer in the double-beam mode with the Wilks cell in the front beam and a ND filter, with an optical density of 0.65, placed in the back beam. All vapor pressures were monitored using a high-vacuum diaphragm manometer (Varian DV100) coupled to a pressure gauge (Varian model 6543−25−039). Room temperature vapor-phase spectra in the $\Delta v_{SH} = 5$ region of *tert*-butylthiol were also recorded with intracavity laser photoacoustic spectroscopy (ICL-PAS). The setup has been described elsewhere.[62,63] The ICL-PAS spectra were recorded with a tunable titanium:sapphire laser (Coherent 890) with a short-wave output coupler, which covered the region from approximately 11 240 to 14 700 cm^{-1}. The line width of the titanium:sapphire laser is approximately 1 cm^{-1}. In our photoacoustic cell we use Knowles EK3133 microphones to detect the photoacoustic signal.

Analysis of the experimental spectra yielded oscillator strengths, *f*, obtained using the following equation[64,65]

$$f = 2.6935 \times 10^{-9}(\mathrm{K^{-1}Torr\ m\ cm})\frac{T}{pl}\int A(\tilde{\nu})\mathrm{d}\tilde{\nu} \quad (1)$$

where T is the temperature of the sample, p is the sample pressure in the cell, l is the path length, and A is the absorbance ($\log_{10}$). Because the photoacoustic signal is proportional to absorbance with an unknown constant, absolute absorbance data from the photoacoustic spectra cannot be obtained. We deconvolute each SH-, CH-, or OH-stretching region into a number of Lorentzian bands with a linear baseline with the *Grams* software package to obtain the integrated absorbances.[66]

Theory and Calculations. The geometries of the lowest-energy conformers of ethanethiol, ethanol, *tert*-butylthiol, and *tert*-butanol were optimized using B3LYP hybrid density functional theory and CCSD(T) ab initio theory. The optimization threshold criteria was set to gradient $= 1 \times 10^{-5}$ a.u., stepsize $= 1 \times 10^{-5}$ a.u., energy $= 1 \times 10^{-7}$ a.u. The integration grid-size used for the density functional calculations was set with an overall target accuracy of 1×10^{-8} a.u. The single point CCSD(T) threshold criteria was set to energy $= 1 \times 10^{-8}$ a.u., orbital $= 1 \times 10^{-8}$ a.u., coefficient $= 1 \times 10^{-8}$ a.u. CCSD(T) theory is known to provide accurate molecular geometries and spectroscopic constants provided a suitably large basis set is used.[67] For ethanol and *tert*-butanol, a triple-ζ correlation consistent basis set augmented with diffuse basis functions (aug-cc-pVTZ) was used. For ethanethiol and *tert*-butylthiol, this basis set was supplemented with additional tight d basis functions on the second-row sulfur atoms [aug-cc-pV(T+d)Z].[68] These additional tight d functions have been shown to significantly improve the geometries and energies of sulfur-containing compounds.[25,69−72] The high computational cost of the CCSD(T) method prevented us from using the augmented triple-ζ basis set to treat *tert*-butylthiol. Instead, we have used a composite basis set in which the methyl groups are described by the cc-pVTZ basis set and the remaining C, S, and H atoms by the full aug-cc-pV(T+d)Z basis set. We denote this partially augmented basis set aug'-cc-pV(T+d)Z. We have previously used this basis set methodology to successfully model the weak intramolecular hydrogen bond in ethylene glycol.[29]

We have calculated the enthalpy (ΔH_{298K}), entropy ($T\Delta S_{298K}$) and resulting Gibbs free energy (ΔG_{298K}) of the conformers of ethanol and ethanethiol at 298 K using standard statistical mechanics. We have used the CCSD(T)/aug-cc-pVTZ and CCSD(T)/aug-cc-pV(T+d)Z methods to determine the electronic energy and the B3LYP/aug-cc-pVTZ and B3LYP/aug-cc-pV(T+d)Z methods to determine the rotational constants and harmonic frequencies of the conformers. All calculations were performed with *Molpro 2006.1*.[73]

We calculate the SH- and OH-stretching wavenumbers and oscillator strengths for ethanethiol, ethanol, *tert*-butylthiol, and *tert*-butanol with an anharmonic oscillator local mode model.[1] The OH-stretching modes in a range of molecules have been previously shown to be isolated from other vibrational modes and hence are well described by the local mode model of vibration.[3,19,25,29] The local mode model has previously been applied to the SH-stretching vibrations of hydrogen sulfide.[36] If we assume that the SH- and OH-stretching vibrations can be described by a Morse oscillator, then the vibrational energy levels are given by

$$E(v)/(hc) = \left(v + \frac{1}{2}\right)\tilde{\omega} - \left(v + \frac{1}{2}\right)^2 \tilde{\omega}x \qquad (2)$$

The Morse oscillator frequency $\tilde{\omega}$ and anharmonicity $\tilde{\omega}x$ are found from the 2nd-, 3rd-, and 4th-order derivatives of the potential-energy curve as described previously.[29,74] These derivatives are found by fitting a 12th-order polynomial to a symmetric 13-point ab initio calculated potential-energy curve, obtained by displacing the SH or OH bond from −0.30 to +0.30 Å in 0.05 Å steps around equilibrium. This range and stepsize of the potential-energy curve ensures converged energy derivatives.

The dimensionless oscillator strength f of a transition from the ground vibrational state g to an excited vibrational state e is given by[7,64]

$$f = 4.702 \times 10^{-7}[\text{cm D}^{-2}]\tilde{\nu}_{eg}|\vec{\mu}_{eg}|^2 \qquad (3)$$

where $\tilde{\nu}_{eg}$ is the transition frequency in cm^{-1} and $\vec{\mu}_{eg} = \langle e|\vec{\mu}|g\rangle$ is the transition dipole moment in Debye (D). We can expand the transition dipole moment matrix element as

$$\langle v|\mu|0\rangle = \frac{\partial\mu}{\partial q}\langle v|q|0\rangle + \frac{1}{2}\frac{\partial^2\mu}{\partial q^2}\langle v|q^2|0\rangle + \frac{1}{6}\frac{\partial^3\mu}{\partial q^3}\langle v|q^3|0\rangle + \ldots \qquad (4)$$

where q is the internal vibrational displacement coordinate. The integrals $\langle v|q^n|0\rangle$ required for the transition dipole moment were evaluated analytically.[75] The dipole moment coefficients are found by fitting a 6th-order polynomial to a 15-point dipole moment curve, obtained by displacing the SH or OH bond from −0.30 to +0.40 Å in 0.05 Å steps around equilibrium.[28]

Results and Discussion

Geometries. In Table 1, we present selected geometric parameters of the experimental and CCSD(T) optimized structures of ethanethiol and *tert*-butylthiol. We find the gauche and trans conformers of ethanethiol optimized with the CCSD(T)/aug-cc-pV(T+d)Z method are in good agreement with the structures determined from microwave spectroscopy.[52,54] Rotational constants obtained using both the B3LYP and CCSD(T) optimized geometries of gauche and trans ethanethiol and *tert*-butylthiol are in good agreement with rotational constants determined by microwave spectroscopy (Tables S1 and S2 of the Supporting Information). The dipole moments of gauche and trans ethanethiol are calculated to be 1.634 and 1.609 D respectively with the CCSD(T)/aug-cc-pV(T+d)Z method. These calculated dipole moments are within the uncertainty limits of the experimentally determined values of 1.61 ± 0.05 D and 1.58 ± 0.04 D for the gauche and trans conformers, respectively.[53]

We have calculated harmonic frequencies for gauche and trans ethanethiol and *tert*-butylthiol with the B3LYP/aug-cc-pV(T+d)Z method. These calculated frequencies are available in Tables S3−S5 of the Supporting Information. We find there to be no imaginary frequencies for the conformers of ethanethiol and *tert*-butylthiol, confirming that our structures correspond to true minima on the potential-energy surface. We calculate the Gibbs free energy (ΔG_{298K}) difference between trans and gauche ethanethiol to be 161 cm^{-1} (1.92 kJ mol^{-1}). This value is consistent with previously calculated energy differences between the conformers obtained with the B3LYP method.[47,48] An energy difference of 161 cm^{-1} corresponds to a relative abundance of 81% for gauche ethanethiol and 19% for trans ethanethiol at room temperature, after accounting for structural degeneracy. We see absorption features in our vibrational spectra of ethanethiol that correspond to two distinct conformers. The

TABLE 1: Selected Structural Parameters (Bond Lengths in Angstroms and Bond Angles in Degrees) of Ethanethiol and *tert*-Butylthiol

	Calculated		Experiment[a]	
molecule	$\angle_{CCSH}$	R_{SH}	$\angle_{CCSH}$	R_{SH}
tert-butylthiol[b]	180.0	1.3414		
gauche ethanethiol [c]	61.61	1.3408	61.75 (0.96)	1.336 (0.010)
trans ethanethiol[c]	180.0	1.3400	180.0	1.322 (0.006)

[a] Derived from microwave experiments reported by Nakagawa et al.[54] [b] Calculated with the CCSD(T)/aug'-cc-pV(T+d)Z method. [c] Calculated with the CCSD(T)/aug-cc-pV(T+d)Z method.

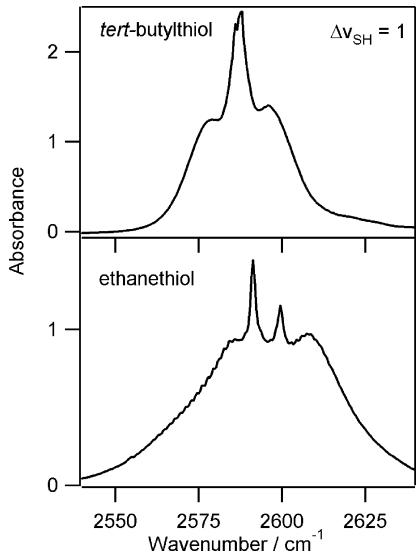

Figure 3. The $\Delta v_{SH} = 1$ transitions of ethanethiol and *tert*-butylthiol recorded with a 15 cm cell and pressures of 402 and 157 Torr, respectively.

TABLE 2: Observed and AO Calculated[a] SH-Stretching Energies (cm^{-1}) and Oscillator Strengths (f) of Ethanethiol[b]

Δv_{SH}	ν_{calcd}	ν_{obs}	f_{calcd}[c]	f_{obs}
1	2591 (2599)	2591 (2599)	8.3×10^{-7}	3.9×10^{-7}
2	5083 (5102)	5084 (5104)[d]	1.9×10^{-8}	1.4×10^{-8}
3	7476 (7508)	7476 (7509)	2.0×10^{-9}	9.0×10^{-10}
4	9770 (9818)		6.7×10^{-11}	
5	11 966 (12031)		2.6×10^{-12}	

[a] Calculations were performed with CCSD(T)/aug-cc-pV(T+d)Z dipole moment functions and experimental local mode parameters. [b] The values for conformers are listed with parentheses for trans and without for gauche. [c] Relative abundances have been accounted for in the f_{calcd} using the Boltzmann distributions of 81% gauche and 19% trans. [d] The expected position of the $\Delta v_{SH} = 2$ band for the trans conformer (text for discussion).

relative intensity of these peaks is consistent with our calculated abundance for the gauche and trans conformers.

SH- vs OH- vs CH-Stretching Intensities. This study compares unperturbed SH-, OH-, and CH-oscillators to quantify differences in the intensity of XH-stretching fundamental and overtone transitions. In Figures 1 and 2, we present overview spectra of ethanethiol and *tert*-butylthiol to give an idea of the relative strengths and frequencies of SH- and CH-oscillators in the near-infrared region. The equivalent overview spectrum of ethanol is given in Figure S1 of the Supporting Information for comparison. It is clear from Figures 1 and 2 that, for a given overtone, CH-stretching transitions are more intense than the equivalent SH-stretching transitions.

In Figures 3−7, we show detailed spectra of the $\Delta v_{SH} = 1-3$ vibrations for ethanethiol and $\Delta v_{SH} = 1-5$ vibrations for *tert*-butylthiol. The observed band positions and intensities of these SH-stretching transitions are given in Tables 2 and 3. The sinusoidal features in the ethanethiol spectra are due to etalon effects and are not a physical characteristic of the molecule. The etalon fringes occur because of interference between the parallel cell windows, which creates wavelength-dependent sinusoidal variation in intensity. The $\Delta v_{CH} = 1-4$ stretching transitions for ethanethiol and *tert*-butylthiol have also been observed and are shown in detail in Figures S2−S5 of the Supporting Information. The observed band positions and intensities of these CH-stretching transitions are included in Tables S6 and S7 of the Supporting Information. The $\Delta v_{CH} = 5$ band of *tert*-butylthiol observed using cavity ringdown spectroscopy is shown in Figure S6 of the Supporting Information.

TABLE 3: Observed and AO Calculated SH-Stretching Energies (cm^{-1}) and Oscillator Strengths (f) of *tert*-Butylthiol[a]

Δv_{SH}	ν_{calcd}	ν_{obs}	f_{calcd}	f_{obs}
1	2587	2588	1.2×10^{-6}	7.1×10^{-7}
2	5076	5075	1.3×10^{-8}	1.6×10^{-8}
3	7466	7465	1.8×10^{-9}	1.7×10^{-9}
4	9756	9756[b]	6.3×10^{-11}	1.6×10^{-10}
5	11 948	11 950[b]	2.4×10^{-12}	

[a] Calculated with a CCSD(T)/aug'-cc-pV(T+d)Z dipole moment function and experimental local mode parameters. [b] Assignment guided by the energy predicted by a Birge−Sponer plot of $\Delta v_{SH} = 1-3$.

In Figure 8, we plot the observed SH- and CH-stretching oscillator strengths of ethanethiol and *tert*-butylthiol and the OH- and CH-stretching oscillator strengths of ethanol and *tert*-butanol. As indicated in the figure inset, SH-oscillators are shown in black, OH-oscillators are shown in blue, and CH-oscillators are shown in red. Our present OH-stretching oscillator strengths are in good agreement with previous work by Lange et al.[16] In the fundamental region, we see that the intensity of the SH-oscillators is smallest, followed by the CH- and OH-oscillators. This order of oscillator strengths continues in the overtone region and becomes even more pronounced with higher degrees of vibrational excitation.

The SH-oscillators possess weak overtones, especially when compared to the relatively strong OH-oscillators. The SH-stretching oscillator strengths of ethanethiol and *tert*-butylthiol are compared with the equivalent OH-stretching oscillator strengths of ethanol and *tert*-butanol in Table 4. Whereas the SH fundamental oscillator strength is on the order of 10^{-7}, the CH oscillator strengths (per CH bond) range between 10^{-7} and 10^{-6} (Tables S6 and S7 of the Supporting Information), and the corresponding OH-stretching fundamental oscillator strengths are on the order of 10^{-6}. Vibrational overtone intensities generally decrease by an order of magnitude with each additional quantum of excitation. We find that the intensity of the SH-stretching vibration drops by roughly a factor of 30 from the fundamental to the first overtone, whereas the CH- and OH-stretching intensities drop by a factor of ~10−20. This variation in the experimentally determined oscillator strengths is mirrored in our calculated XH-stretching oscillator strengths (Tables 2−4). The ratio between the OH- and SH-stretching intensity is significantly less for the fundamental transitions compared to the overtones, reflecting the larger drop in intensity from the fundamental to first overtones for the SH-stretching transition.

Our calculated SH-stretching oscillator strengths for ethanethiol and *tert*-butylthiol are in reasonable agreement with the observed oscillator strengths. Oscillator strengths of CH- and OH-stretching transitions calculated using an AO local mode approach are typically within a factor of 2 of experimentally determined oscillator strengths.[15,19,25,28,76] For the $\Delta v_{SH} = 1-3$ SH-stretching transitions of ethanethiol, we find the theoretical oscillator strengths to be consistently larger (1.4−2.2 times) than the observed oscillator strengths. For *tert*-butylthiol, the calculated oscillator strengths of the $\Delta v_{SH} = 1$ and 3 SH-stretching transitions are also higher than the observed oscillator strengths while the $\Delta v_{SH} = 2$ and 4 SH-stretching transitions are lower than the observed oscillator strengths. It should be noted that

TABLE 4: Observed and AO Calculated SH- and OH-Stretching Oscillator Strengths

		Experimental			Calculated		
molecular fragment	Δv	f(SH)	f(OH)	f(OH):f(SH)	f(SH)	f(OH)	f(OH):f(SH)
ethan-	1	3.9×10^{-7}	2.2×10^{-6}	5.6	8.3×10^{-7} [b,c]	2.4×10^{-6} [c,d]	2.9
	2	1.4×10^{-8}	4.3×10^{-7}	30.7	1.9×10^{-8} [b,c]	5.3×10^{-7} [c,d]	27.9
	3	9.0×10^{-10}	2.2×10^{-8}	24.4	2.0×10^{-9} [b,c]	2.2×10^{-8} [c,d]	11.0
tert-butyl-	1	7.1×10^{-7}	1.8×10^{-6}	2.5	1.2×10^{-6} [e]	1.0×10^{-6} [f]	0.8
	2	2.0×10^{-8}	4.4×10^{-7}	22.0	1.3×10^{-8} [e]	4.0×10^{-7} [f]	30.8
	3	1.7×10^{-9}	2.4×10^{-8}	14.1	1.8×10^{-9} [e]	1.9×10^{-8} [f]	10.6
	4	1.6×10^{-10}	1.9×10^{-9} [a]	11.9	6.3×10^{-11} [e]	1.0×10^{-9} [f]	15.9

[a] From ref 16. [b] Calculated with the CCSD(T)/aug-cc-pV(T+d)Z method. [c] Represented in proportion to the calculated Boltzmann distributions of 81% gauche and 19% trans for ethanethiol and 61% gauche and 39% trans for ethanol. [d] Calculated with the CCSD(T)/aug-cc-pVTZ method. [e] Calculated with the CCSD(T)/aug'-cc-pV(T+d)Z method. [f] Calculated with the CCSD(T)/aug'-cc-pVTZ method.

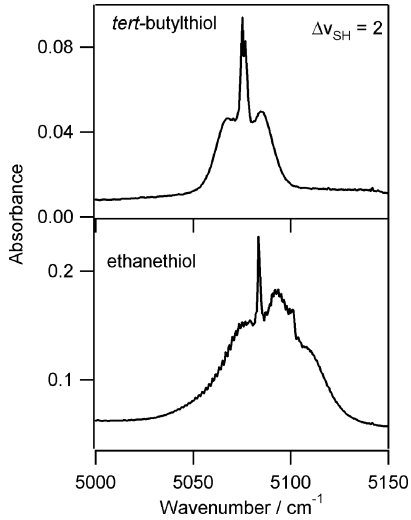

Figure 4. The $\Delta v_{SH} = 2$ transitions of ethanethiol and *tert*-butylthiol, recorded with a 71.4 cm cell and pressures of 460 and 83 Torr, respectively.

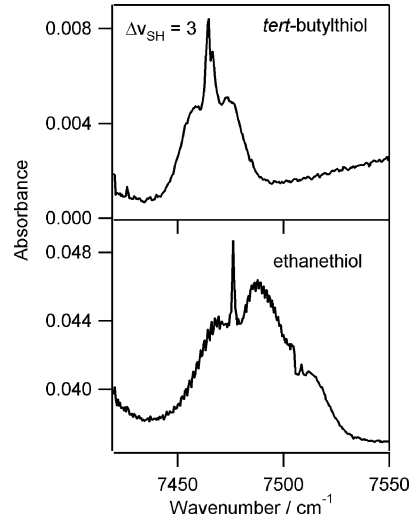

Figure 5. The $\Delta v_{SH} = 3$ transitions of ethanethiol and *tert*-butylthiol, recorded with a 71.4 cm cell and pressures of 460 and 83 Torr, respectively.

the observed oscillator strengths presented in Tables 2 and 3 represent our best experimental results. In Tables S6 and S7 of the Supporting Information, we give experimental oscillator strengths from numerous experiments carried out in both the Boulder and Otago laboratories. For *tert*-butylthiol, our observed oscillator strengths vary by up to 40%, whereas for ethanethiol the range of observed oscillator strengths is as much as 60%.

Uncertainties in the experimental oscillator strengths arise because of inaccuracies in the sample vapor pressure and problems with deconvoluting overlapping bands. These experimental difficulties are apparent from the range of intensities obtained for the various bands from different experiments. Although we have directly measured the vapor pressure used to fill the cell, some experiments used glass bodied cells, which easily become coated by sample. The measured vapor pressure is thus likely overestimated and the oscillator strength underestimated. Other experiments utilized metal long pass Wilks cells with a much lower surface area to path length ratio and as a result have more reliable vapor-pressure measurements.

The coupling of the bright SH-stretching states to the bath of dark states complicated the measurement of the intensity of the inherently weak SH-stretching transitions for the higher overtones ($\Delta v_{SH} \geq 4$). In this region the CH stretch−bend combination transitions are likely to be of comparable intensity to the SH-stretching transitions and thus the dark states will carry significant intensity by themselves. This is apparent in Figure 6 in which the SH-stretching transition is not the strongest peak in the band. We have reported the intensity of the $\Delta v_{SH} =$ 4 transition in *tert*-butylthiol as the area of the deconvoluted Lorentzian associated with the peak at 9756 cm^{-1}.

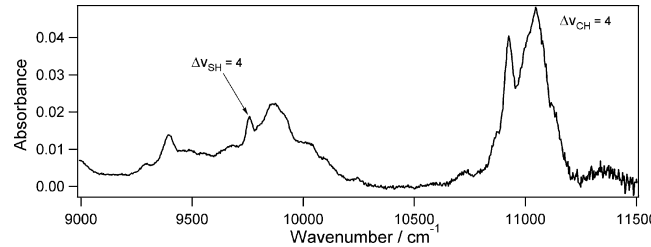

Figure 6. The $\Delta v_{SH} = 4$ and $\Delta v_{CH} = 4$ transitions of *tert*-butylthiol, recorded with a 14.25 m cell and a pressure of 102 Torr.

Two factors govern intensities of vibrational local mode transitions: the anharmonicity of the local mode oscillator and the derivatives of the dipole moment function along the local mode coordinate. To that end, we use a local mode AO model to explain the observed paucity of the SH-stretching transitions when compared with OH-stretching transitions. The calculated and experimentally derived local mode parameters of the SH bonds in the alkanethiols studied are given in Table 5, and those of the corresponding alcohols in Table S8 of the Supporting Information. For the $\Delta v_{SH} = 2$ band of ethanethiol, the Q-branch of the gauche conformer is easily identified, whereas the Q-branch of the less-abundant trans conformer is difficult to assign and is omitted from our Birge−Sponer fit. The $\Delta v_{SH} =$ 2 transition is tentatively assigned to 5104 cm^{-1}, which fits well with the experimentally determined local mode parameters. For both molecules, the uncertainty on the calculated local mode

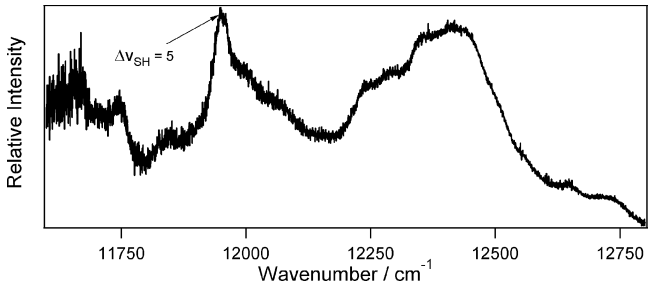

Figure 7. The $\Delta v_{SH} = 5$ transition of *tert*-butylthiol, recorded with ICL-PAS spectroscopy. The spectrum was recorded at 57 Torr.

TABLE 5: Calculated[a] and Observed Local Mode Parameters $\tilde{\omega}$ and $\tilde{\omega}x$ (cm^{-1})

	Observed		Calculated	
	$\tilde{\omega}$	$\tilde{\omega}x$	$\tilde{\omega}$	$\tilde{\omega}x$
gauche ethanethiol	2690.2 ± 0.3[b]	49.51 ± 0.08[b]	2697.15	49.54
trans ethanethiol	2695.6[c]	48.21[c]	2704.73	49.44
tert-butylthiol	2686.4 ± 0.7[d]	49.45 ± 0.16[d]	2693.46	49.47

[a] Calculated with the CCSD(T)/aug-cc-pV(T+d)Z method for ethanethiol and the CCSD(T)/aug'-cc-pV(T+d)Z method for *tert*-butylthiol. [b] Obtained by a Birge−Sponer fit of the $\Delta v_{SH} = 1-3$ stretching frequencies observed in Boulder. [c] Obtained by a Birge−Sponer fit of the $\Delta v_{SH} = 1$ and $\Delta v_{SH} = 3$ stretching frequencies observed in Boulder. [d] Obtained by a Birge−Sponer fit of the $\Delta v_{SH} = 1-5$ stretching frequencies observed in Otago.

parameters is low, confirming the assignments. We find that the experimental and theoretical SH-stretching anharmonicities ($\tilde{\omega}x$) are within one wavenumber of each other at the CCSD(T) level of theory whereas the theoretical local mode frequencies ($\tilde{\omega}$) obtained with the same method are ~10 cm^{-1} higher than those determined from experiment. This agreement between the experimental and theoretical local mode parameters is consistent with some of our recent studies of OH-stretching oscillators at the CCSD(T) level of theory.[25,29] We find that the B3LYP calculated local mode frequency of each alkanethiol is in excellent agreement (less than 1 cm^{-1}) with the SH-stretching harmonic frequency obtained using a normal mode model (Tables S3−S5 and S9 of the Supporting Information). This indicates that the SH-stretching vibrational modes are localized and are well described by an AO local mode model.

TABLE 6: CCSD(T) Dipole Moment Derivatives of Ethanethiol, Ethanol, *tert*-Butylthiol and *tert*-Butanol[a]

	gauche ethan		trans ethan		*tert*-butyl	
order	SH	OH	SH	OH	SH	OH
0	1.6336	1.7249	1.6094	1.6002	1.6677	1.6220
1	0.2836	0.5999	0.3036	0.6432	0.3479	0.4291
2	0.5637	1.1112	0.6308	1.2736	0.5761	1.1453
3	0.2082	1.1929	0.2407	1.3448	0.1892	1.0737
4	0.3740	0.0319	0.4081	0.0349	0.3822	0.0656
5	0.2705	0.8118	0.3059	0.9479	0.2790	0.7892
6	0.3131	0.1587	0.3469	0.1869	0.3240	0.1526

[a] All values given in Debye. The derivatives given are the square root of the sum of the three squared components.

The anharmonicity of the SH-stretching local mode in ethanethiol and in *tert*-butylthiol is ~49 cm^{-1}, which is significantly less than typical anharmonicities of OH-, NH-, and CH- stretching oscillators.[1] The anharmonicity of the OH-stretching local mode in ethanol and in *tert*-butanol is ~85 cm^{-1} (Table S8 of the Supporting Information) and thus based on anharmonicity arguments one would expect the SH-stretching intensities to be significantly weaker than corresponding OH-stretching intensities. A smaller anharmonicity is expected to lead to smaller transition intensity due to the size of the integrals involved in eq 4.[77]

The oscillator strength of a fundamental transition is determined predominantly by the first term in the expansion of eq 4, that is the first derivative of the dipole moment function. The integral over the coordinate multiplied by the frequency of the local mode is almost identical for a SH- and OH-stretching vibration and hence the relative intensity of the fundamental transition depends almost entirely on the difference in the first derivative of the dipole moment function. For overtone transitions, several terms contribute to the intensities of vibrational overtone transitions.[78,79] This can lead to near cancellation of terms for the first overtone and hence a wide variation in the intensity of the $\Delta v_{SH} = 2$ transition.

The calculated dipole moment derivatives of the SH- and OH-stretching modes are very different. In Table 6, we present the CCSD(T) calculated dipole moment derivatives of ethanethiol, ethanol, *tert*-butylthiol, and *tert*-butanol. In general, we find that

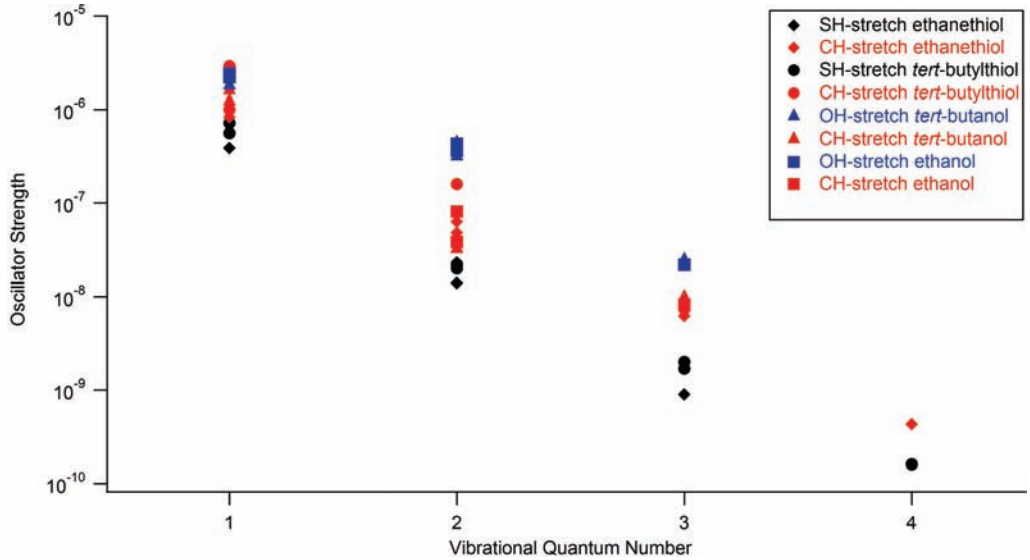

Figure 8. Experimentally determined SH-stretching (black), OH-stretching (blue), and CH-stretching (red) oscillator strengths for ethanethiol, ethanol, *tert*-butylthiol, and *tert*-butanol.

the first three derivatives of the SH-oscillators are smaller than those of the corresponding OH-oscillators. This leads to significantly weaker fundamental SH-stretching transitions corroborating our present experimental results and in agreement with previous H_2O and H_2S intensities.[35−37] The SH-stretching mode is more harmonic than the OH-stretching mode and as such one would expect the SH-stretching overtone transitions to become increasingly weaker. However, the matrix elements in eq 4 calculated for the OH and SH oscillator respectively show that the SH overlaps are larger. These larger overlap integrals partially compensate for the smaller anharmonicity of the SH-oscillators. We have also calculated oscillator strengths of the SH-stretching transitions with SH local mode parameters and both the SH and OH dipole moment derivatives. Likewise, we have calculated the OH-stretching intensities with OH local mode parameters and both the OH and the SH dipole moment derivatives. Comparison of these calculations illustrates that the intensity of the fundamental XH-stretching transitions is primarily determined by the derivatives of the dipole moment function. Whereas the effect of anharmonicity becomes greater for the overtone transition intensities, we find that the dipole moment function continues to dominate the resulting intensity.

Conclusions

Vapor-phase SH-stretching overtone spectra have been recorded in the $\Delta v_{SH} = 1-3$ regions for ethanethiol and $\Delta v_{SH} = 1-5$ regions for *tert*-butylthiol to investigate the unperturbed SH-oscillator local mode. We compare these SH-stretching transitions with CH-stretching transitions from the aforementioned alkanethiols and OH-stretching transitions from the corresponding alcohols, ethanol, and *tert*-butanol. We observe paucity in the intensity of the SH-stretching transitions during this comparison. The SH-stretching fundamental and overtone intensities are approximately an order of magnitude less intense than the OH-stretching transitions of the corresponding alcohols. We explain the observed weak intensity in the SH-stretching fundamental and overtone transitions using high-level ab initio calculations and an anharmonic oscillator local mode model. We find that the anharmonicity of the SH-oscillators is around half the value of the OH-oscillators studied in this work. The low anharmonicity of the SH-stretching vibrational modes contributes increasingly to the low intensities of the SH-stretching overtones. However, the paucity of intensity of the fundamental and overtone SH-stretching transitions cannot be explained by the low anharmonicity alone. We observe that the variation in the dipole moment function is the most important factor in determining the intensities of these alkanethiols.

Acknowledgment. We thank K. Takahaski, A.L. Garden, and S.J. Lind for helpful discussions. M.E.D. acknowledges funding from the NASA NESSF program. We acknowledge funding from the NSF and the Marsden Fund administered by the Royal Society of New Zealand.

Supporting Information Available: Spectra showing the $\Delta v_{CH} = 2 - 4$ transitions of ethanethiol; spectra showing the $\Delta v_{CH} = 1-5$ transitions of *tert*-butylthiol; the spectrum of ethanol between 4500 cm^{-1} and 11 500 cm^{-1}; B3LYP/aug-cc-pV(T+d)Z calculated harmonic frequencies of all of the alkanethiols studied in this work; calculated and experimental rotational constants for both ethanethiol and *tert*-butylthiol in tabular form; observed CH-stretching intensities of ethanethiol and *tert*-butylthiol in tabular form; frequencies and intensities of the alkanethiols determined with different experimental conditions in tabular form; calculated and observed local mode parameters of ethanol. This material is available free of charge via the Internet at http://pubs.acs.org.

References and Notes

(1) Henry, B. R. *Acc. Chem. Res.* **1977**, *10*, 207.
(2) Henry, B. R. *Acc. Chem. Res.* **1987**, *20*, 429.
(3) Henry, B. R.; Kjaergaard, H. G. *Can. J. Chem.* **2002**, *80*, 1635.
(4) Mortensen, O. S.; Henry, B. R.; Mohammadi, M. A. *J. Chem. Phys.* **1981**, *75*, 4800.
(5) Child, M. S. *Acc. Chem. Res.* **1985**, *18*, 45.
(6) Child, M. S.; Halonen, L. *Adv. Chem. Phys.* **1984**, *57*, 1.
(7) Kjaergaard, H. G.; Yu, H.; Schattka, B. J.; Henry, B. R.; Tarr, A. W. *J. Chem. Phys.* **1990**, *93*, 6239.
(8) Quack, M. *Annu. Rev. Phys. Chem.* **1990**, *41*, 839.
(9) Halonen, L. *Adv. Chem. Phys.* **1998**, *104*, 41.
(10) Kjaergaard, H. G.; Henry, B. R. *J. Chem. Phys.* **1992**, *96*, 4841.
(11) Kjaergaard, H. G.; Henry, B. R. *J. Phys. Chem.* **1995**, *99*, 899.
(12) Kjaergaard, H. G.; Henry, B. R.; Tarr, A. W. *J. Chem. Phys.* **1991**, *94*, 5844.
(13) Kjaergaard, H. G.; Proos, R. J.; Turnbull, D. M.; Henry, B. R. *J. Phys. Chem.* **1996**, *100*, 19273.
(14) Kjaergaard, H. G.; Turnbull, D. M.; Henry, B. R. *J. Phys. Chem. A* **1997**, *101*, 2589.
(15) Phillips, J. A.; Orlando, J. J.; Tyndall, G. S.; Vaida, V. *Chem. Phys. Lett.* **1998**, *296*, 377.
(16) Lange, K. R.; Wells, N. P.; Plegge, K. S.; Phillips, J. A. *J. Phys. Chem. A.* **2001**, *105*, 3481.
(17) Takahashi, K.; Sugawara, M.; Yabushita, S. *J. Phys. Chem. A* **2002**, *106*, 2676.
(18) Takahashi, K.; Sugawara, M.; Yabushita, S. *J. Phys. Chem. A* **2003**, *107*, 11092.
(19) Donaldson, D. J.; Orlando, J. J.; Amann, S.; Tyndall, G. S.; Proos, R. J.; Henry, B. R.; Vaida, V. *J. Phys. Chem. A* **1998**, *102*, 5171.
(20) Hintze, P. E.; Kjaergaard, H. G.; Vaida, V.; Burkholder, J. B. *J. Phys. Chem. A* **2003**, *107*, 1112.
(21) Donaldson, D. J.; Tuck, A. F.; Vaida, V. *Chem. Rev.* **2003**, *103*, 4717.
(22) Havey, D. K.; Vaida, V. *J. Mol. Spectrosc.* **2004**, *228*, 152.
(23) Vaida, V.; Feierabend, K. J.; Rontu, N.; Takahashi, K. *Int. J. Photoenergy* **2008**, *2008*.
(24) Havey, D. K.; Feierabend, K. J.; Takahashi, K.; Skodje, R. T.; Vaida, V. *J. Phys. Chem. A* **2006**, *110*, 6439.
(25) Lane, J. R.; Kjaergaard, H. G.; Plath, K. L.; Vaida, V. *J. Phys. Chem. A* **2007**, *111*, 5434.
(26) Kjaergaard, H. G.; Henry, B. R. *Mol. Phys.* **1994**, *83*, 1099.
(27) Kjaergaard, H. G.; Daub, C. D.; Henry, B. R. *Mol. Phys.* **1997**, *90*, 201.
(28) Rong, Z.; Henry, B. R.; Robinson, T. W.; Kjaergaard, H. G. *J. Phys. Chem. A* **2005**, *109*, 1033.
(29) Howard, D. L.; Jørgensen, P.; Kjaergaard, H. G. *J. Am. Chem. Soc.* **2005**, *127*, 17096.
(30) Lane, J. R. *Application of Electronic Structure Calculations to Atmospheric Trace Species*; Otago University: Dunedin, New Zealand, 2008.
(31) Niefer, B. I.; Kjaergaard, H. G.; Henry, B. R. *J. Chem. Phys.* **1993**, *99*, 5682.
(32) Howard, D. L.; Robinson, T. W.; Fraser, A.; Kjaergaard, H. G. *Phys. Chem. Chem. Phys.* **2004**, *6*, 719.
(33) Fehrensen, B.; Hippler, M.; Quack, M. *Chem. Phys. Lett.* **1998**, *298*, 320.
(34) Krikorian, S. E.; Mahpour, M. *Spectrochim. Acta A* **1973**, *29*, 1233.
(35) Bykov, A. D.; Naumenko, O. V.; Smirnov, M. A.; Sinitsa, L. N.; Brown, L. R.; Crisp, J.; Crisp, D. *Can. J. Phys.* **1994**, *72*.
(36) Vaittinen, O.; Biennier, L.; Campargue, A.; Flaud, J. M.; Halonen, L. *J. Mol. Spectrosc.* **1997**, *184*, 288.
(37) Naumenko, O.; Campargue, A. *J. Mol. Spectrosc.* **2001**, *209*, 242.
(38) Wolff, H.; Szydlowski, J. *Can. J. Chem.* **1985**, *63*, 5.
(39) Sheppard, N. *J. Chem. Phys.* **1949**, *17*, 5.
(40) Manocha, A. S.; Fateley, W. G.; Shimanouchi, T. *J. Phys. Chem.* **1973**, *77*, 1977.
(41) Barnes, A. J.; Hallam, H. E.; Howells, J. D. R. *Trans. Faraday Soc.* **1972**, 7.
(42) Trotter, I. F.; Thompson, H. W. *J. Chem. Soc.* **1946**, *1946*, 481.
(43) Smith, D.; Devlin, J. P.; Scott, D. W. *J. Mol. Spectrosc.* **1968**, *25*, 11.
(44) Allinger, N. L.; Fan, Y. *J. Comput. Chem.* **1997**, *18*, 21.
(45) Durig, J. R.; Bucy, W. E.; Wurrey, C. J. *J. Phys. Chem.* **1975**, *79*, 6.
(46) Ohsaku, M.; Ichiishi, T.; Imamura, A.; Hayashi, M. *Bull. Chem. Soc. Jpn.* **1984**, *57*, 6.

(47) Takahashi, K. *XH Stretching Vibrational Spectra, A Theoretical Perspective*; Keio University: Tokyo, 2004.
(48) Choi, S.; Kang, T. Y.; Choi, K.-W.; Han, S.; Ahn, D.-S.; Baek, S. J.; Kim, S. K. *J. Phys. Chem. A.* **2008**, *112*, 9.
(49) McCullough, J. P.; Hubbard, W. N.; Frow, F. R.; Hossenlopp, I. A.; Waddington, G. *J. Am. Chem. Soc.* **1957**, *79*, 6.
(50) Richter, W.; Schiel, D. *Chem. Phys. Lett.* **1984**, *108*, 4.
(51) Rosei, M. A. *Physiol. Chem. Phys. Med. NMR* **1988**, *20*, 189.
(52) Hayashi, M.; Imaishi, H.; Ohno, K.; Murata, H. *Bull. Chem. Soc. Jpn.* **1970**, *43*, 1.
(53) Schmidt, R. E.; Quade, C. R. *J. Chem. Phys.* **1975**, *62*, 3864.
(54) Nakagawa, J.; Kuwada, K.; Hayashi, M. *Bull. Chem. Soc. Jpn.* **1976**, *49*, 13.
(55) Valenzuela, E. A.; Woods, R. C. *J. Chem. Phys.* **1974**, *61*, 10.
(56) Margules, L.; Hartwig, H.; Mader, H.; Dreizler, H.; Demaison, J. *J. Mol. Struct.* **1998**, *517*−*518*, 387.
(57) Allinger, N. L.; Hickey, M. J. *J. Am. Chem. Soc.* **1975**, *97*, 11.
(58) Fausto, R.; Teixeira-Dias, J. J. C.; Carey, P. R. *J. Mol. Struct.* **1987**, *159*, 16.
(59) Sosa, C.; Bartlett, R. J.; KuBulat, K.; Person, W. B. *J. Phys. Chem.* **1989**, *93*, 12.
(60) Hameka, H. F. *Phosphorous Sulfur* **1990**, *53*, 373.
(61) Brown, S. S. *Chem. Rev.* **2003**, *103*, 5219.
(62) Henry, B. R.; Kjaergaard, H. G.; Niefer, B.; Schattka, B. J.; Turnbull, D. M. *Can. J. Appl. Spectrosc.* **1993**, *38*, 42.
(63) Rong, Z.; Kjaergaard, H. G. *J. Phys. Chem. A* **2002**, *106*, 6242.
(64) Atkins, P. W.; Friedman, R. S. *Molecular Quantum Mechanics*, 3rd ed.; Oxford University Press: Oxford, 1997.
(65) Waldrom, R. J.; Kuschel, M.; Kjaergaard, H. G.; Henry, B. R. *J. Phys. Chem. A* **2006**, *110*, 913.
(66) Grams/AI, version 8.0, Thermo Fischer Scientific Inc.
(67) Helgaker, T.; Ruden, T. A.; Jorgensen, P.; Olsen, J.; Klopper, W. *J. Phys. Org. Chem.* **2004**, *17*, 479.
(68) Dunning, T. H. J.; Peterson, K. A.; Wilson, A. K. *J. Chem. Phys.* **2001**, *114*, 9244.
(69) Wilson, A. K.; Dunning, T. H., Jr. *J. Chem. Phys.* **2003**, *119*, 11712.
(70) Garden, A. L.; Lane, J. R.; Kjaergaard, H. G. *J. Chem. Phys.* **2006**, *125*, 144317.
(71) Lane, J. R.; Kjaergaard, H. G. *J. Phys. Chem. A.* **2008**, *112*, 4958.
(72) Lane, J. R.; Kjaergaard, H. G. *J. Phys. Chem. A* **2007**, *111*, 9707.
(73) A Werner, H.-J. K. , P. J.; Lindh, R.; Manby, F. R.; Schutz, M.; Celani, P.; Korona, T.; Rauhut, G.; Amos, R. D.; Bernhardsson, A.; Berning, A.; Cooper, D. L.; Deegan, M. J. O.; Dobbyn, A. J.; Eckert, F.; Hampel, C.; Hetzer, G.; Lloyd, A. W.; McNicholas, S. J.; Meyer, W.; Mura, M. E.; Nicklass, A.; Palmieri, P.; Pitzer, R.; Schumann, U.; Stoll, H.; Stone, A. J.; Tarroni, R.; Thorsteinsson, T. *MOLPRO*, version 2006.1, a package of ab initio programs, 2006.
(74) Herzberg, G. *Molecular Spectra and Molecular Structure I. Spectra of Diatomic Molecules*; Van, D., Ed.; Nostrand Company, Inc.: Princeton, NJ, 1950.
(75) Rong, Z.; Cavagnat, D.; Lespade, L. *Lecture Notes in Computer Science*; Springer-Verlag: Berlin, 2003; Vol. 2658.
(76) Brown, S. S.; Wilson, R. W.; Ravishankara, A. R. *J. Phys. Chem. A* **2000**, *104*, 4976.
(77) Low, G. R.; Kjaergaard, H. G. *J. Chem. Phys.* **1999**, *110*, 9104.
(78) Kjaergaard, H. G.; Henry, B. R. *J. Chem. Phys.* **1992**, *96*, 4841.
(79) Kjaergaard, H. G.; Low, G. R.; Robinson, T. W.; Howard, D. L. *J. Phys. Chem. A* **2002**, *106*, 8955.

JP9017162